PROBLEMY KOLEJNICTWA
RAILWAY REPORT
Issue 195 (June 2022)
DOI: 10.36137/1954E
ISSN 0552-2145 (print) ISSN 2544-9451 (on-line)

Thermal Phenomena Related to Plastic Deformation During Tensile Testing and Their Microscopic Interpretation

Małgorzata OSTROMĘCKA[1], Jakub SIWIEC[2]

Summary
Thermal phenomena related to plastic deformation can be commonly observed. By simply touching a ruptured or bent sample, it is clear that the temperature has risen at the deformation site. Such observations can be carried out for qualitative or quantitative assessment. This paper serves to qualitatively relate the changes in the structure of the deformed material to the temperature increase observed with an infrared camera.

Keywords: strain of materials, heat generation, tensile test, dissimilar joint, friction welding

1. Introduction

The static tensile test of metals is one of the basic and most frequently performed tests of the strength of materials due, among other reasons, to the fact that the deformation and fracture of construction materials are of constant interest to many researchers. At the Railway Research Institute, the static tensile test is carried out at room temperature in numerous tests of construction elements or materials of railway components. The tests are carried out in accordance with the recommendations of ISO 6892-1:2016-09 using method B [1]. The result of a static tensile test is usually the determination of one or more of the specified quantities:

- the (conventional) yield point,
- ultimate tensile strength,
- tensile stresses,
- elongation,
- necking.

In terms of the standard tests performed in the industry, the Institute rarely analyses phenomena that involve heat emission during material deformation, although it is not difficult to experience them - after rupture, a metal sample is hot at the point of fracture. The objective of this paper is to present the results of a static tensile test of a friction-welded dissimilar joint, supplemented by infrared camera observation and interpretation of the accompanying deformation mechanisms.

2. Description of selected phenomena occurring during plastic deformation

Basically, two extreme cases can be presented: quasi-static deformation and dynamic deformation. In quasi-static deformation, there is a state of static equilibrium at every instant, i.e. the sum of the forces acting on each part of the deformed element is close to zero, so this case can be considered as a sequence of equilibrium states described by the equations of materials mechanics. In contrast, in high-speed loading, when a force acts on one part of the component and another part does not "feel it", this means that the stress "travels" through the component at a certain speed as a wave. Depending on the deformation (strain) rate, three scenarios involving heat emission can be presented:

- the heat released during the process is conducted through the device components and the environment and dissipates so that the body remains practically isothermal (low deformation (strain) rate);
- the process is virtually adiabatic, as there is insufficient time for the generated heat to dissipate (dynamic deformation processes);

[1] Ph.D., Eng.; Railway Research Institute, Materials & Structure Laboratory; e-mail: mostromecka@ikolej.pl.
[2] M.Sc. Eng.; Railway Research Institute, Materials & Structure Laboratory; email: jsiwiec@ikolej.pl.

- the process involves heat generation as well as heat dissipation (intermediate state – average deformation (strain) rates) [2].

The thermal processes accompanying deformation are directly related to the deformation mechanism, and with an increase in deformation (strain) rate, there is a change from slipping, through controlled slipping and through activated processes, to viscoplastic flow.

According to current knowledge [3], the basic mechanism of plastic deformation of crystalline materials is the irreversible movement of dislocations in slip planes (Figure 1). In addition, under certain conditions, e.g. at high temperature, atomic displacements can occur due to diffusive mass transport or slipping across grain boundaries. Crystals that do not have a sufficient number of independent slip systems deform by twinning in addition to slipping. As a result of local shearing in the deformed region (twin), the orientation of the crystal structure changes to a specular reflection of the undeformed structure (Fig. 2).

The final stage of the deformation process is a fracture, the course of which is largely determined by the nature of the earlier deformation. It therefore depends on the type of material and its properties, and therefore results not only from mechanical, but also thermal, magnetic and other stresses. The direction of maximum stress and type of tensile fracture are shown in Table 1. Depending on the macroscopic orientation of the scrap surface, it is possible to distinguish the following:

- detachment (brittle fracture) (Fig. 3a),
- shearing (ductile fracture) (Fig. 3b).

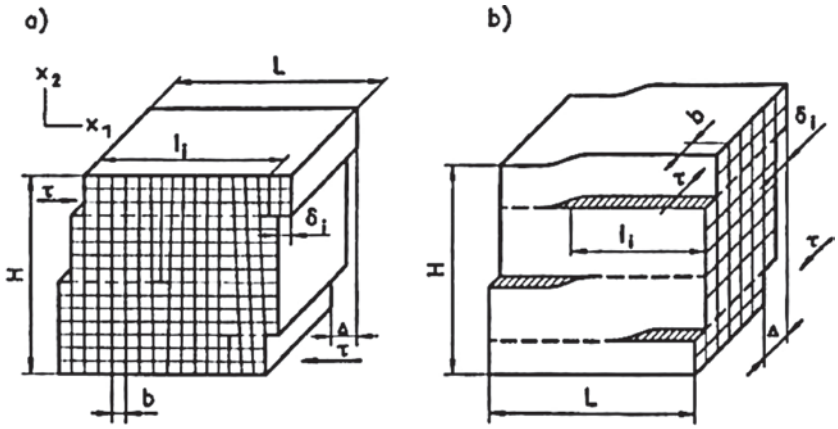

Fig. 1. Crystal deformation after the passage of dislocations [3]: a) edge; b) screw

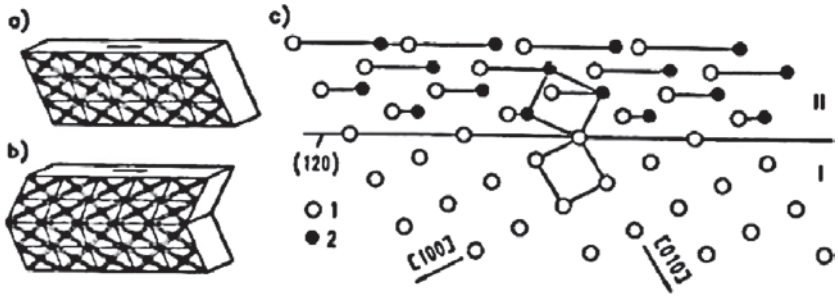

Fig. 2. Schematic of plastic deformation of a crystal of regular lattice by twinning [4]: a) undeformed crystal, b) crystal after twinning, c) geometry of twinning along the plane of twinning (120); I – untwinned part of the crystal, II – twinned part of the crystal, ○ – Initial position of atoms, ● – position of atoms after twinning

Table 1

Direction of maximum stress and type of tensile fracture [4]

Loading method		Direction of maximum stresses		Type of fracture	
		Normal	tangential	detachment	shearing
Tensile testing					

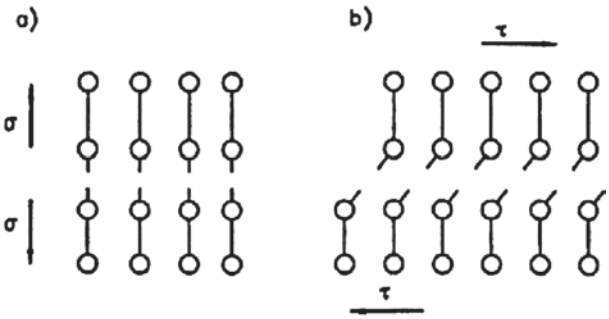

Fig. 3. Scheme of atomic bond rupture [3]: a) in detachment, where the interaction of normal tensile stresses results in the rupture of atomic bonds in the fracture plane, oriented perpendicular to the stress direction; b) in shearing, which occurs due to the rupture of atomic bonds under tangential stresses in the fracture plane parallel to the stress direction by transverse or longitudinal shearing

In the case of metals, a perfectly brittle detachment is not obtained, and very small plastic deformations precede the fracture.

3. Research materials and methodology

The subjects of the study were friction welded joints, according to the developed welding technology, made between a ribbed bar of B500B reinforcing steel and martensitic alloy steel 1.4021 (2H13). The chemical compositions of the parent materials are given in Tables 2 and 3 and the welding parameters in Table 4.

The test stand (Figs. 4, 5) consisted of an Instron Schenck Testing Systems LFV universal testing machine with a maximum load of 5000 kN with a computer-controlled measurement and control console and a camera: FLIR ONE (measurement limit error ±3°C or 5%).

Fig. 4. Test stand – universal testing machine [photo: M. Ostromęcka]

Table 2

Chemical composition of reinforcing steel (parent material 1)

Reinforcing steel B500B	C [%]	N [%]	S [%]	P [%]	Cu [%]	Carbon equivalent C_{eq}
	≤ 0.24	≤ 0.013	≤ 0.055	≤ 0.055	≤ 0.85	≤ 0.52

[On the basis of the attached approvals].

Table 2

Chemical composition of martensitic steel (parent material 2)

Steel 1.4021 (2H13)	C [%]	Mn [%]	Si [%]	P [%]	S [%]	Cr [%]	Ni [%]	Cu [%]
	0.16 – 0.25	< 1.5	< 1.0	< 0.04	< 0.03	12.0 – 14.0	–	–

[On the basis of the attached approvals].

Table 3

Welding parameters

Rotational speed n [rpm]	Pressure force F_t [kG/cm²]	Upsetting force F_s [kG/cm²]	Friction time t_t [s]	Upsetting time t_s [s]	Welding area [mm²]
800	115	140	5	6	490

[On the basis of the developed welding technology].

Fig. 5. Camera set up before the study [photo: M. Ostromęcka]

Tensile testing of the samples was carried out at 27°C ±1°C at a rate determined from EN ISO 6892-1 clause 10.3.3 (*Testing rate based on stress rate – method B*), Table 3 – materials with a modulus of E ≥ 150 GPa. The rate of load build-up was 30 MPa/s. The obtained results were used to determine the tensile strength of the joint and to observe thermal phenomena in the qualitative assessment. It should be noted that the joints were subjected to tension without any special preparation, including the removal of the flash.

Metallographic specimens for observing the microstructure of the joint were prepared using Struers' Rotopol-22 grinder-polisher. The samples were ground with diamond grinding discs of gradations: 80, 120, 600, 1200, and finally polished with a 1 μm diameter polycrystalline diamond slurry made by Buehler. Etching was carried out with 4% Nital reagent and Adler's reagent. Detailed descriptions of the procedures used in the preparation of samples for macroscopic and microscopic examination are described in a separate paper [5]. The microstructure was observed using a KEYENCE VHX-900F digital microscope.

4. Discussion of the results

The base material on the side of the reinforcing bar had a perlitic-ferritic structure, which fragmented upon moving closer to the weld line. On both sides of the weld, a thermo-plastic zone with characteristically aligned lines was visible. On the type 1.4021 steel side, the structure in the immediate vicinity of the weld was very fine and, as it moved away from the weld line, the grains became larger and consisted of lath martensite. The weld itself was very narrow, typical of a friction welding process. On the martensitic steel side, an unfavourable fibrous structure was observed, which could have had a significant impact on the fracture pattern (Figure 6).

Fig. 6. Microstructure of the dissimilar welded joint between B500B and 1.4021 steel; on the left the microstructure of the B500B reinforcing steel, on the right the structure of the martensitic steel with distinct fibrousness; microstructure in the initial state before tension [photo: M. Ostromęcka]

During the static tensile test, rupture of sample B22.5/21 occurred after 26.5 seconds at a maximum breaking force of 327.28. The fracture was brittle-plastic in nature, with a significant predominance of brittleness and no necking. The flash from both welded materials remained adhered to the martensitic part of the joint, which may indicate that the fracture occurred in the thermo-plastic zone in the immediate vicinity of the weld on the reinforcing steel side. Photographs of the ruptured sample are shown in Figures 7 and 8. The calculated tensile strength for this sample was 668 MPa. This was the value corresponding to the strength indicated in the approval for B500B reinforcing steel. The joint therefore handled the expected loads.

In the case of sample B23.4/21, rupture occurred after 26.8 seconds with a maximum rupture force of 302.09. The fracture was also brittle-plastic in nature, with a significant preponderance of brittleness and lack of necking; however, the flash was ruptured in the axis of the weld, which may suggest that the most weakened area of the joint, however, was the

weld itself. It is likely that in the process, bonding occurred with insufficient material mixing of the two steels. Photographs of the ruptured sample are shown in Figures 9 and 10. The calculated tensile strength for this sample was 616MPa. This was approximately 10% lower than the strength value indicated on the approval for B500B reinforcing steel. The results obtained are presented in Table 5.

Fig. 7. Sample B22.5/21 after the test [photo: M. Ostromęcka]

Fig. 8. Fracture of the weld in sample B22.5/21 [photo: M. Ostromęcka]

Fig. 9. Sample B23.4/21 after the test [photo: M. Ostromęcka]

Fig. 10. Fracture of the weld in sample B23.4/21 [photo: M. Ostromęcka]

Figure 11 shows the shape of the load-displacement relationship in sample B23.4/21. The course of this graph indicates that the transition from elastic deformation (range from O to A) to plastic deformation (from point B) is a complex process and a so-called "flow section" (AB) is formed on the deformation

Table 5

Results obtained for selected samples during tensile tests

Sample marking	Initial cross-sectional area [mm²]	Max. breaking force Fm [kN]	Tensile strength Rm [MPa]	Rupture site
B22.5/21	490	327.28	668	weld in the thermo-plastic zone on the reinforcing steel side
B22.5/21	490	302.09	616	in the weld

[Own elaboration].

curve. The length of this section is called the Lüders band. The range of the curve between points B and C represents the plastic deformation (irreversible) that ends with the sample rupturing at point C. The load-displacement relationship for both test samples had a similar shape, with differences only in the position of the characteristic points. In the case of sample B23.4/21, the stress initiating the flow process was approximately 260 kN. This phenomenon was not preceded by the occurrence of a "tooth" of flow (a markedly higher value of the upper yield point relative to the lower yield point). This stress is highly dependent on the presence of stress concentrators and the height of the flow ‚tooth' decreases when the material's ductility is compromised and inclusions are present.

In sample B22.5/21, no ‚tooth' of flow was observed either, but the Lüders stress was higher, at around 280 kN. The course of the load-displacement relationship for both samples confirmed the existence of a certain initial state of internal stresses, which had a form consistent with the expectations of the authors of the study. Plastic deformation starts once the elastic limit is exceeded. Further increases in stress generate new dislocations and increase the stress field around existing dislocations. Once the upper yield point is reached near stress concentrators (such as grain boundaries, secondary phase particles, inclusions, etc.), the generation of ‚new' dislocations is rapid. During the generation of such a dislocation, there is a drop in stress to the lower yield point, which is a condition for plastic flow. The graphs (Figs. 12, 14) show the load-time relationships for samples B22.5/21 and B23.4/21 recorded in tension at a load build-up rate of 30 MPa/s. The individual points marked on the graphs correspond to frames from films shot with a thermographic camera (Figures 13 and 15). The frames were carefully selected

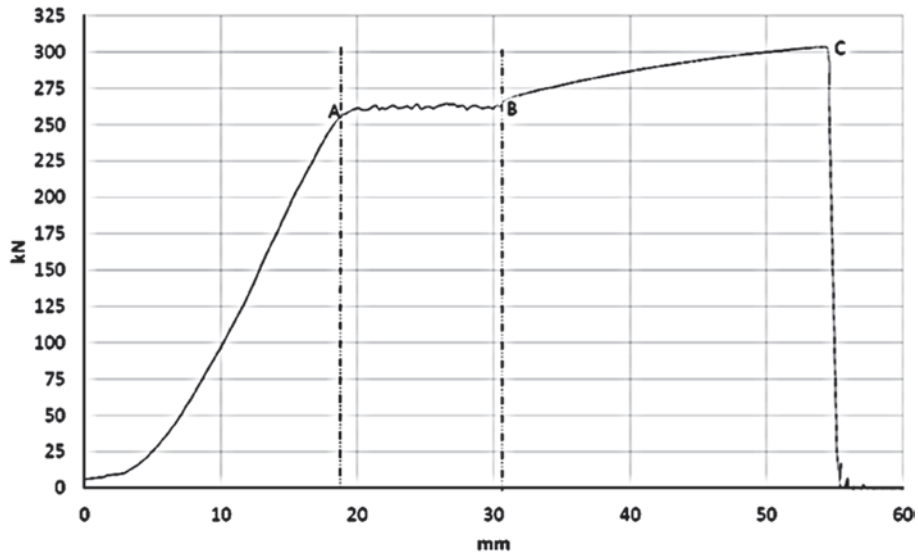

Fig. 11. Shape of load-displacement relationship in sample B23.4/21, OA – elastic range; AB – flow; BC – plastic deformation range; C – sample rupture [elaborated by J. Siwiec]

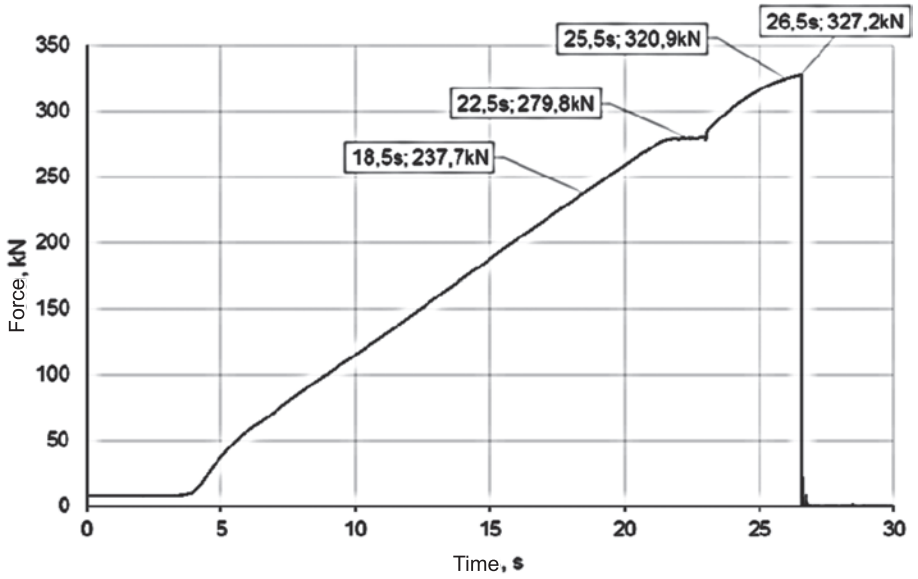

Fig. 12. Load-time relationship in sample B22.5/21 [elaborated by J. Siwiec]

to show the response of the material in the elastic range, during flow, in the plastic range and at rupture. As the starting temperature of the tensile samples was relatively high (27–28°C), since the test was carried out in the summer season, no clear change in temperature in relation to the ambient temperature was recorded in the frames of Figures 13 and 15a, 15b. The frames (Figures 15c, 15d) show the state recorded in terms of plastic deformation. The contrast of the frame shows a clear difference in the temperature of the samples compared to the ambient temperature. It should be noted that, in each case, the temperature at the rupture site continued to rise after the sample was ruptured, with the observed temperature rise reaching over 38°C.

It is noteworthy that the highest temperatures were recorded on the reinforcing bar side, which is the ‚weaker' material and it is in this area that rupture was predicted. The increase in temperature in this area was manifested

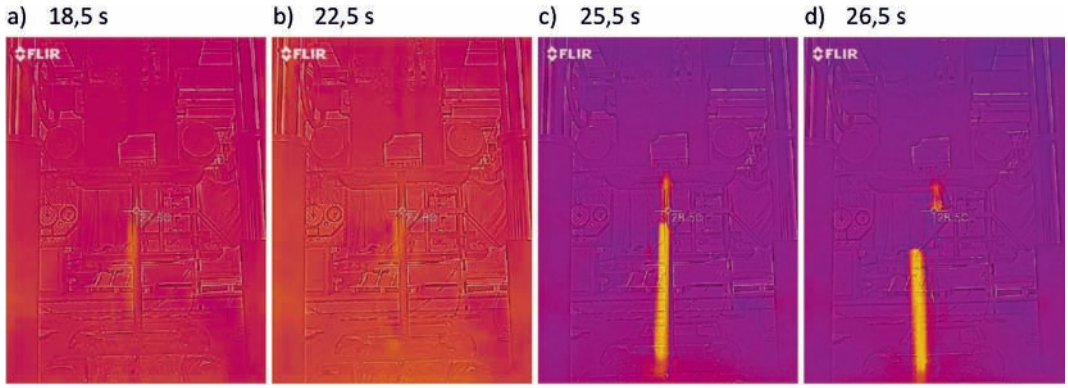

Fig. 13. Images from the thermographic camera in successive seconds of the recording for sample B22.5/21 [taken by J. Siwiec]

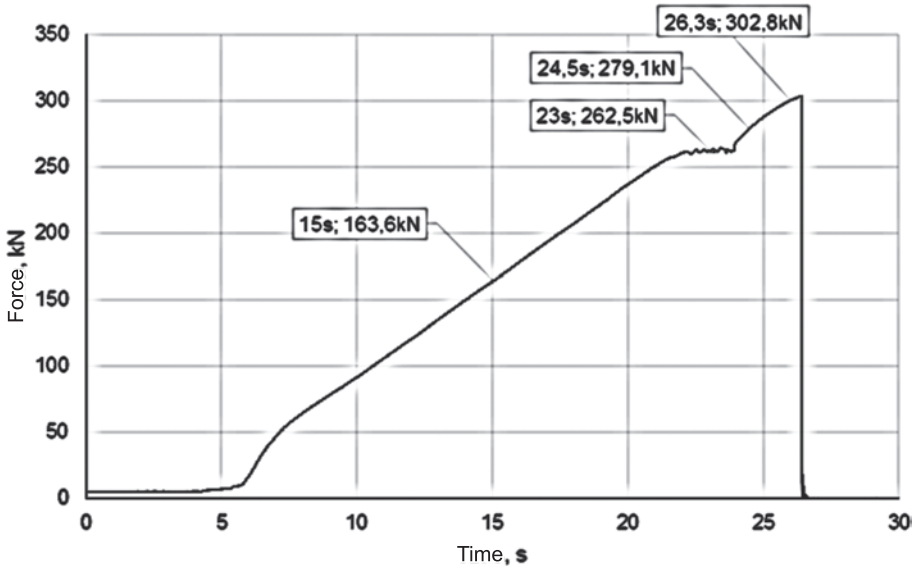

Fig. 14. Load-time relationship in sample B23.4/21 [elaborated by J. Siwiec]

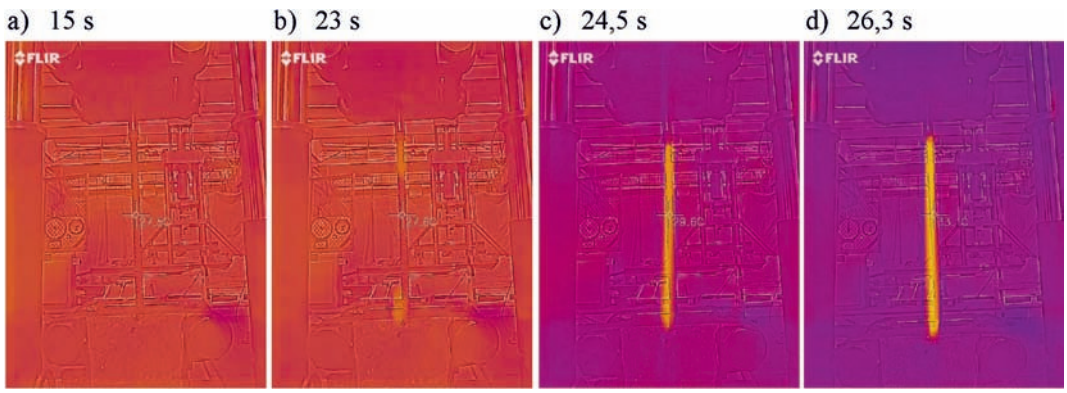

Fig. 15. Images from the thermographic camera in successive seconds of the recording for sample B22.5/21 [taken by J. Siwiec]

on the film frame by an intense yellow colour, contrasting clearly with the purple background of the surroundings. Observations confirmed that heat is generated during deformation and it is spread dynamically, although it proceeds with some delay, which is related to the applied deformation (strain) rate and thermal conductivity.

In a polycrystalline material plastically deformed at room temperature, the development of the microstructure is examined from the perspective of the development of dislocation systems, due to their higher (in comparison to point defects) energy. The processes of dislocation formation and movement, as well as the interactions between dislocations and other elements of the microstructure, significantly influence the process of energy storage and material strengthening. The change in the temperature field in the material undergoing deformation is a macroscopic manifestation of phenomena occurring at the microstructural level.

The total energy w used to deform the material is equal to the work of elastic deformation w_e (reversible) and the work of plastic deformation w_p (irreversible) according to the formula:

$$w = w_e + w_p.$$

Plastic deformation energy is combined with heat dispersion q_d and energy storage in the material e_s. Therefore:

$$w = w_e + q_d + e_s.$$

All these values were related to a unit of the working mass of the sample, which means that they are relevant values.

If one examines the quasi-static deformation process of a material by relating it to the thermodynamic state of an unloaded annealed sample, the principles of classical thermodynamics can be used to describe the tensile test carried out for the purposes of this paper [6]. However, the samples we examined already exhibited a certain state of internal stress related to the dissimilar materials' welding process (friction welding). This condition was evident by the fibrousness of the structure arranged perpendicular to the direction of tension. At the atomic level, this is linked to the existence of significant disorder in the crystal structure, which means that configurational entropy can have a significant impact during deformation. For quasi-static processes, in homogeneous materials in the annealed state, the configurational entropy is neglected; however, the static tensile test performed as part of the present study was conducted at a medium tensile speed and the material had a structural notch inside – a weld and numerous stress concentrators. For this reason, the process could be observed at a qualitative level, and calculating the heat released in the process associated with the temperature change would not contribute any constructive quantitative information.

5. Conclusion

The observation of thermal phenomena during a static tensile test at a qualitative level is an additional source of information on the location and mechanism of plastic deformation. In the case of dissimilar welded joints, analysis of the thermogram at a qualitative level can make it easier to pinpoint the point of rupture, which is not at all obvious in the case of very thin areas such as the weld. Analysis of the infrared camera film also provides a fairly clear indication of which material is more prone to plastic deformation. Graphs normally produced during a static tensile test do not provide such information.

For qualitative observations, it is possible to examine samples without special preparation. Thus, it may be expedient to use this method when testing finished products or railway components such as railway couplings.

References

1. EN ISO 6892-1:2016-09: Metallic materials – Tensile testing – Part 1: Method of test at room temperature
2. Kyzioł L.: *Wpływ temperatury i szybkości odkształcania na charakterystyki wytrzymałościowe materiałów metalicznych* [Influence of temperature and rate of deformation on the strength characteristics of metallic materials], Zeszyty Naukowe Akademii Morskiej w Gdyni, 2017, number 100, p. 109–119.
3. Wyrzykowski J.W., Pleszakow E., Sieniawski J.: *Odkształcenie i pękanie metali* [Metal deformation and fracture], Wydawnictwo Naukowo-Techniczne PWN, Warszawa, 1999.
4. Hertzberg R.W.: *Deformation and fracture mechanics of engineering materials*, J. Wiley and Sons, New York – Toronto, 1998.
5. Ostromęcka M., Szymański M.: *Preparatyka zgładów do badań makro- i mikroskopowych pochodzących ze zgrzewanych tarciowo złączy różnoimiennych stalowych oraz ich ocena w odniesieniu do obowiązujący norm* [Preparation of specimens for macro and microscopic examinations of dissimilar friction welded steel joints and their evaluation according to applicable standards], Problemy Kolejnictwa, 2022, p. 195.
6. Maj M.: *Wpływ wstępnego odkształcenia na proces magazynowania energii w polikryształach* [The influence of initial deformation on the process of energy storage in polycrystals], rozprawa doktorska, Instytut Podstawowych Problemów Techniki Polskiej Akademii Nauk IPPT PAN, Warszawa, 2007.